

LETTER • OPEN ACCESS

Cyclone Fani: the tug-of-war between regional warming and anthropogenic aerosol effects

To cite this article: Lin Zhao *et al* 2020 *Environ. Res. Lett.* **15** 094020

View the [article online](#) for updates and enhancements.

Environmental Research Letters



LETTER

Cyclone Fani: the tug-of-war between regional warming and anthropogenic aerosol effects

OPEN ACCESS

RECEIVED
17 October 2019

REVISED
8 April 2020

ACCEPTED FOR PUBLICATION
11 May 2020

PUBLISHED
19 August 2020

Original content from this work may be used under the terms of the [Creative Commons Attribution 4.0 licence](#).

Any further distribution of this work must maintain attribution to the author(s) and the title of the work, journal citation and DOI.



Lin Zhao^{1,2} , S-Y Simon Wang² , Emily Becker³, Jin-Ho Yoon⁴  and Avik Mukherjee²

¹ Key Laboratory of Land Surface Process and Climate Change in Cold and Arid Regions, Northwest Institute of Eco-Environment and Resources, Chinese Academy of Sciences, Lanzhou, People's Republic of China

² Department of Plants, Soils and Climate/Utah Climate Center, Utah State University, Logan, UT, United States of America

³ University of Miami Rosenstiel School of Marine and Atmospheric Science, Miami, FL, United States of America

⁴ School of Earth Sciences and Environmental Engineering, Gwangju Institute of Science and Technology, Gwangju, Republic of Korea

E-mail: yjinho@gist.ac.kr

Keywords: cyclone Fani, WRF-Chem, anthropogenic aerosols, regional climate warming

Supplementary material for this article is available [online](#)

Abstract

Before Cyclone Amphan took place in 2020, Cyclone Fani (May 2019) is the strongest pre-monsoon cyclone in the Bay of Bengal (BOB) since 1991, killing 90 people in eastern India and Bangladesh while causing US\$1.81 billion of damages. Fani developed during a period of high concentration of anthropogenic aerosols in the BOB with abnormally high sea surface temperature (SST), thereby presenting an opportunity to understand the compound effects of atmospheric aerosols and regional climate warming on a tropical cyclone. A quantitative attribution analysis was conducted using the Weather Research and Forecasting model with chemistry (WRF-Chem) run at the convection-permitting (4 km) grid spacing, accompanied by an ensemble of coarser-resolution simulations to quantify the uncertainty. The removal of post-1990 trends in the tropospheric variables and SST from WRF-Chem's initial conditions (IC) and boundary conditions (BC, including the lateral and lower boundary conditions) resulted in a reduction of cyclone precipitation by about 51% during the 5 d of April 28–May 2. The removal of tropospheric warming shows approximately twice as strong an effect on Fani (39% reduction in precipitation) as that of SST warming (22% reduction). When aerosol's direct and indirect effects were removed from the simulations, i.e., no aerosol influence on radiation and cloud microphysics, Fani initially strengthened but later weakened, as measured by geopotential height and precipitation amounts. These results suggest that aerosol and its interaction with the atmosphere acted to mitigate the strengthening effect of anthropogenic warming on Fani, but was not strong enough to entirely counteract it. Although the ensemble of coarser simulations appears to overestimate Cyclone Fani in terms of precipitation, the direction of the effects is in agreement with that obtained from the 4 km simulations. Given the increasing anthropogenic aerosols in the BOB, future attribution studies using more sophisticated dynamical aerosol models on BOB tropical cyclones are urged.

1. Introduction

Originated from a tropical depression that formed west of Sumatra in the Indian Ocean on 26 April 2019, cyclone Fani eventually developed to the strongest pre-monsoon cyclone (A Category 4-equivalent cyclone in figure 1(a)) in the Bay of Bengal (BOB) since 1991. According to Aon's Weather, Climate & Catastrophe Insight: 2019 Annual Report, Cyclone Fani made landfall in the Indian state of Odisha on 3 May 2019, killing 81 people while causing damages

approximated to 8.1 billion US dollars in Bangladesh and India (www.aon.com). Exposed to a high concentration of anthropogenic aerosols during the pre-monsoon season (Wang *et al* 2013), BOB tropical cyclones are facing a double-punch effect from anthropogenic climate change: persistent warming in the ocean surface and the air, accompanied by a detectable increase in aerosol loading (Bhat *et al* 2001). Literature shows that local climate warming has increased the intensity of BOB cyclones (Yu and Wang 2009, Hoarau *et al* 2012) while a modeling

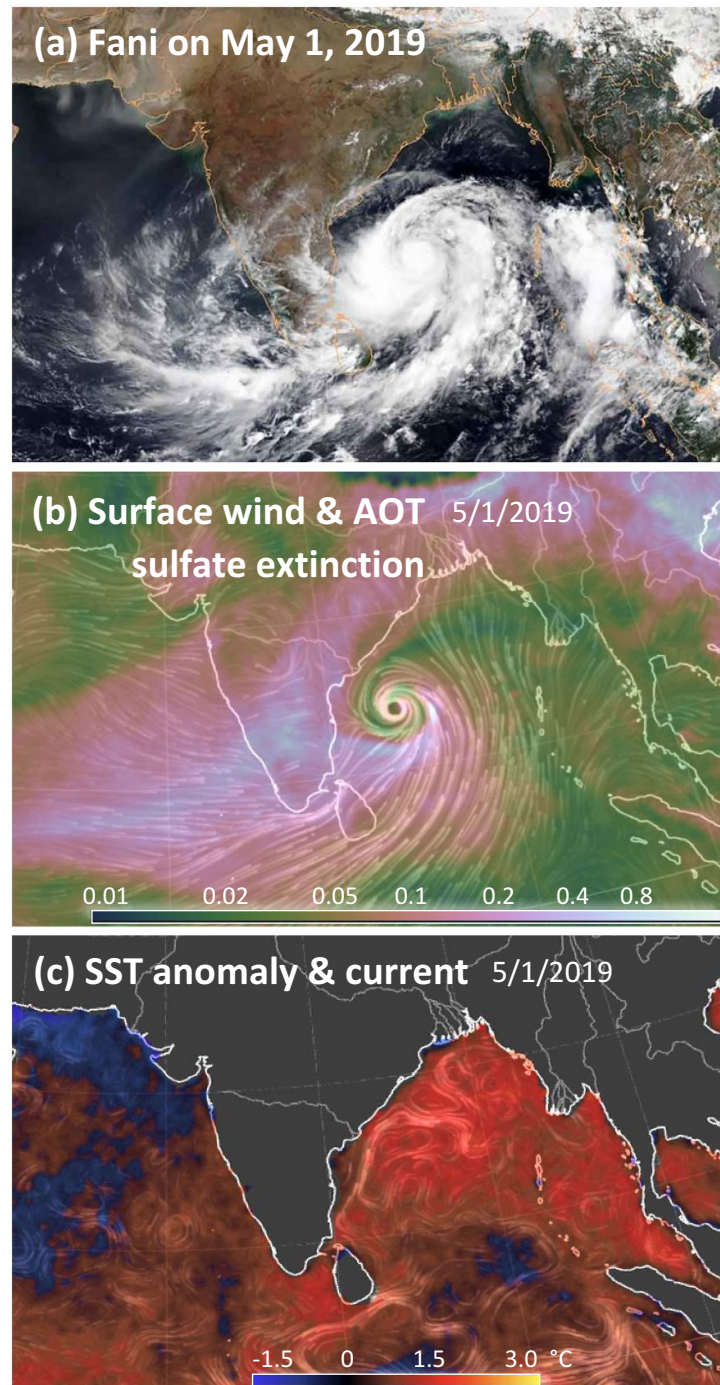


Figure 1. (a) Visible/true-color image of cyclone Fani on 00Z 1 May 2019 depicted by Terra—MODIS (source: NOAA), (b) nullschool generated streamlines of surface wind and the aerosol optical thickness (AOT; shading) by sulfate extinction and (c) SST anomaly overlaid with surface currents (white streamlines) at the same time (source: <https://earth.nullschool.net> with permission).

analysis found that increased aerosols can deepen the short-wave trough that develops in May, subsequently intensifying tropical cyclones during the pre-monsoon season (Wang *et al* 2013). Cyclone Fani developed around the equator as depression and slowly move upward, then it has a quick intensification as an extremely severe cyclonic storm during the 24 h from 0530Z 30th April to 0530Z May 1st, the maximum sustained surface wind speed increased from 120–130 km h⁻¹ to 180–190 km h⁻¹ (<http://www.rsmcnewdelhi.imd.gov.in>). Thus, the

quick intensification of Fani presents an interesting case in understanding the compound effects of atmospheric aerosols and climate warming in the BOB on a pre-monsoon tropical cyclone.

High values of aerosol optical thickness (AOT)¹ due to sulfate extinction were present in the BOB around Cyclone Fani (figure 1(b)), concurrent with

¹AOT is derived from the GEOS-5 data provided by the Global Modeling and Assimilation Office (GMAO) at NASA Goddard Space Flight Center, displayed by <https://earth.nullschool.net>.

intense warm sea surface temperature (SST)² anomalies in the northern BOB, with regions of the ocean reaching 32 °C prior to Fani's landfall (figure 1(c)). In the weather timescale, aerosols present both a negative and positive impact on the microphysical and dynamical properties of clouds: a negative impact is caused by processes that reduce precipitation efficiency (Tao *et al* 2012, Hazra *et al* 2013) and weaken the cyclone winds (Rosenfield *et al* 2012), while a positive impact is associated with the 'cloud invigoration effect' linking an increase in aerosol loading with deepening of convective clouds. The debate about the invigoration effect and possible cloud responses remains fierce, however, as conclusions vary regionally, and depend on aerosol types (Altaratz *et al* 2014, Varble 2018, Jiang *et al* 2018, Fan *et al* 2018). As reported by Evan *et al* (2011), anthropogenic black carbon and sulfate aerosols would reduce the vertical wind shear to create an environment more favorable for tropical cyclone intensification, while Lau and Kim (2007) found that the loading of dust aerosol in the atmosphere might cool SST to suppress the development of cyclone.

During the pre-monsoon season in the BOB, the observed increases in anthropogenic aerosols and ocean heat content may have complex effects on Fani, and understanding these effects requires a novel event attribution analysis. This study does not focus on detailing the aerosol effects on cloud microphysics and convective processes, as that itself is an active research topic (see a review by Fan *et al* 2016). Rather, we seek to provide an attribution analysis that assesses the compound effects of highly concentrated aerosols and persistent SST warming, both of which are present in the BOB during Cyclone Fani.

2. Background of attribution on individual cyclones

Few studies have discussed the effect of climate change on individual tropical cyclones. Due to the large natural variability and the limited period of consistent observations, there is no consensus on how climate change affects the intensity and track of individual tropical cyclones (Landsea *et al* 2006, Patricola and Wehner 2018). The few diagnostic and modeling studies that attributed the effect of climate change on individual tropical cyclones in the recent years point to a general intensification effect on tropical cyclones but with various degrees of rainfall or wind speed change. For example, statistical analysis and modeling experiments have indicated that the warming trend likely intensifies Hurricane Harvey's precipitation by 15%–20% (Risser and Wehner 2017, Van Oldenborgh *et al* 2017, Wang *et al* 2018), enhances

Super Typhoon Haiyan by about 20% (Takayabu *et al* 2015), and strengthens rainfall for Hurricane Florence by 2%–9% (Reed *et al* 2020). In general, the Clausius–Clapeyron (CC) relation that increases moisture holding capacity under climate warming plays a key role in the overall increase of precipitation. However, most previous studies found that the response of tropical cyclone (TC) rainfall to climate warming exceeds the CC relation. (Lenderink *et al* 2017) suggested that both higher moisture content and higher vertical velocities contribute to the TC precipitation process. Adding to the challenges in attributing climate change on individual storms, global climate models have a common difficulty in directly representing tropical cyclones. Therefore, recent studies such as Wehner *et al* (2017), Patricola and Wehner (2018), and (Wang *et al* 2018) urged the need for applying convection-permitting regional simulations for the attribution analysis of hurricanes.

The impact of aerosol on tropical cyclones has mostly been investigated independent of the studies on regional climate warming effects. Using the assimilation of aerosol optical depth, the effects of dust on increasing static stability produce a less favorable environment to tropical cyclogenesis (Reale *et al* 2014). By comparing the effects of aerosol radiative forcing and greenhouse gas on the TC potential intensity, aerosol cooling seems to reduce TC intensity more strongly than greenhouse gas warming increases it (Sobel *et al* 2019). Given the high concentration of anthropogenic aerosols in the BOB, what would these effects be on Fani?

3. Model experiments and data sources

Following the emerging 'storyline approach' of attribution analysis (e.g. Zappa and Shepherd 2017, Wang *et al* 2018), we adopted a quantitative attribution approach that constrains the boundary and initial conditions of a regional atmospheric model used to simulate this synoptic event. Using the Weather Research and Forecasting model with chemistry (WRF-Chem), we can generate the closest possible influences of the environmental conditions at the time of Cyclone Fani (via initial and boundary conditions) and simulate the same event by assuming the absence of long-term (warming) trends in those conditions and of the aerosol effects, in order to examine their combined effects on a TC. We used the WRF-Chem version 3.9.1 that includes aerosol interactions with the atmosphere (Grell *et al* 2005, Skamarock *et al* 2008, Powers *et al* 2017). WRF-Chem utilizes the Modal Aerosol Dynamics for Europe (MADE) aerosol module and Carbon-Bond Mechanism version Z (CBM-Z) to parameterize aerosol transport and deposition and represent the gas-phase chemistry (Ackermann *et al* 1998, Zaveri and Peters 1999). The domain of simulations is composed of 623 × 539 grid points (outlined in figure

² SST is derived from the NOAA Real-time, global, sea surface temperature (RTG_SST_HR) analysis, displayed by <https://earth.nullschool.net>.

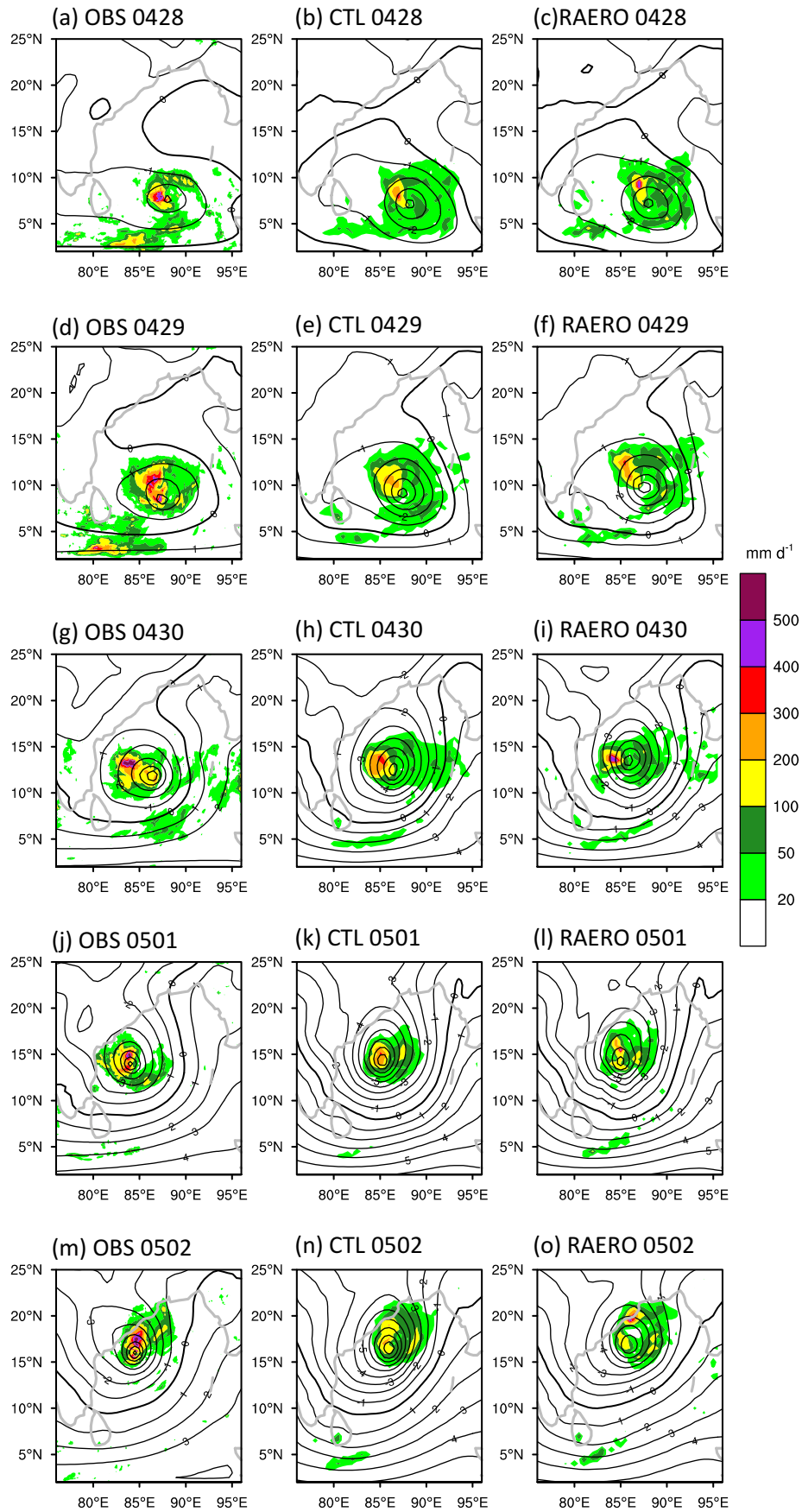


Figure 2. The observed and simulated 850 hPa streamfunction ($\text{m}^2 \text{s}^{-1}$, contours at intervals of $10^7 \text{ m}^2 \text{ s}^{-1}$) at 00UTC overlaid with daily averaged precipitation (mm d^{-1} , shading) within the simulation domain from 28 april to 2 may: (a), (d), (g), (j) and (m) are observation; (b), (e), (h), (h) and (n) are control simulations (CTL); (c), (f), (i), (l) and (o) are simulations without anthropogenic aerosol effects (RAERO).

2) with a horizontal grid spacing of 4 km, a resolution that starts to resolve convective precipitation (i.e. convection-permitting) while convective parameterization is turned off. The model was forced by initial conditions (IC) and boundary conditions (BC, including the lateral and lower boundary conditions) using the $0.5^\circ \times 0.5^\circ$ resolution Global Forecast System (GFS) initial analysis with nesting. Here, SST is derived from GFS rather than other observed data. As reported by Fu and Wang (2018), SST from GFS is a best lower boundary condition for WRF to represent the intensity of typhoon Nangka compared with the NOAA optimum interpolation SST (OISST), and ECMWF Interim reanalysis (ERA-Interim). We conducted four sets of 4 km simulation based on the combination of Lin (Lin *et al* 1983)/Morrison (Morrison *et al* 2009) microphysics schemes with Mellor–Yamada–Nakanishi–Niino (MYNN) (Nakanishi and Niino 2006)/the Yonsei University (YSU) planetary boundary layer (PBL) schemes (Hong *et al* 2006), and subsequently produced the control simulation (CTL, table 1) from their ensemble mean. To quantify model uncertainty, we also conducted multiple simulations with coarser resolution settings to increase the ensemble size. The ensemble spread and members are discussed in section 4.

Based upon Cho *et al* (2016) and Wang *et al* (2016), the regional model experiments were designed under the assumption that any post-1990 trend manifest in the tropospheric and ocean temperatures contains signals that are traceable to the anthropogenic global warming. Since GFS data only started in 2004 (<https://www.ncdc.noaa.gov/data-access/model-data/model-datasets/global-forecast-system-gfs>), which is not adequate for computing the post-1990 trends, we used the NCEP Reanalysis 2 trend given that NCEP GFS also contributes to the NCEP reanalysis (Campana *et al* 2019). We first conducted four experiments of anthropogenic global warming effects with the chemistry component engaged (see table 2): a control simulation (1) forced by the original GFS analysis as IC and BC (CTL, as a 4-member ensemble), and ‘detrended’ simulations in which we removed the linear monthly trends from the IC and BC for (2) SST (denoted as DSST), (3) all tropospheric variables, such as temperature, geopotential height, relative humidity, U wind and V wind (DAIR), and (4) both SST and tropospheric variables (DALL). The trends were first computed from the NCEP-DOE Reanalysis 2 monthly data for each variable (Kanamitsu *et al* 2002) and then linearly interpolated onto GFS’s horizontal and vertical grids. We then subtracted these trends from the GFS’s initial analysis (including geopotential height, horizontal winds, air temperature, etc to be consistent), before using it as IC and BC to drive the WRF-Chem. We note that the individual trends revealed in the different IC and BC

variables may not be linearly correlated but the non-linear effect among these different trends is negligible (not shown). More details about the detrend processes can be referred to Cho *et al* (2016) and Wang *et al* (2016), (2018).

Here, the anthropogenic emission was based on the Emissions Database for Global Atmospheric Research (EDGAR) HTAP V2 inventory (Janssens-Maenhout *et al* 2015). The EDGAR HTAP emission inventory provides total emissions, as well as sector-by-sector estimates for air, energy, industry, residential, shipping, and transportation sectors. To compare the non-anthropogenic aerosol effect on meteorological variables, four additional experiments with non-anthropogenic aerosol effects were designed: (5) a control aerosol simulation forced by the original GFS analysis as IC and BC without aerosols (RAERO; with the chemistry module turned off) and within this setup, a ‘detrend’ experiment of (6) SST (DSST_RAERO), (7) tropospheric variables (DAIR_RAERO), and (8) both SST and tropospheric variables as above (DALL_RAERO), all of which without simulating the interaction between anthropogenic aerosol and the atmospheric variables. However, due to the absence of aerosols, the direct and indirect effects like aerosol-radiation and aerosol-microphysics interaction are not present in these (5)–(8) simulations. To evaluate the sensitivity of the climate trend effect, we also included another three ‘double-trend’ simulations forced by the original IC and BC added with the post-1990 monthly trends (thus doubling the warming effect, i.e. DB run): (9) the atmospheric variables (DBAIR_RAERO), (10) SST (DBSST_RAERO), and (11) both the atmosphere and SST (DBALL_RAERO). We have tested certain runs (RAERO) using both a single domain and a nesting domain with the chemistry component turned off. The results show that both runs can capture the main pattern of the observed precipitation (figures S2 and S3 (available online at stacks.iop.org/ERL/15/094020/mmedia)), which is indicated by the pattern correlation of precipitation between simulations and observation. It is arguable that the lateral boundary interpolated from 50 km to 4 km is not problematic for this simulation domain.

Table 2 provides a summary of these experiments, while the detailed model setup is described in (Wang *et al* 2016). Other physics schemes were configured identically in all simulations, with the following common options: YSU PBL scheme, the NOAA land-surface model (Chen and Dudhia 2001), and the Morrison microphysics scheme. The Fu-Liou-Gu (Fu and Liou 1992, Gu *et al* 2011) radiation scheme, which allows for aerosols in long-wave and short-wave radiation, was applied for the simulations. The additional coarser-resolution simulations (to create a large ensemble) used a combination of other physics

schemes not listed above. All simulations cover the period from 0000 UTC 26 April to 0000 UTC 04 May 2019.

The observed gridded 12 h and daily mean precipitation, derived from Level-3 half-hourly Integrated Multi-satellite Retrievals of Global Precipitation Measurement (IMERG) final product at the $0.1^\circ \times 0.1^\circ$ resolution, was obtained from NASA Global Precipitation Measurement (GPM) data products (<https://pmm.nasa.gov/>). For observed SST, we use the Reynolds SST Analysis (Reynolds *et al* 2007).

4. Results

The observed evolution of Fani from 28 April 2019 to 2 May is displayed in figure 2 (left column) in terms of 850 hPa streamfunction at 00 UTC, overlaid with the daily mean precipitation. Pre-monsoon tropical cyclones in the BOB tend to develop from low-pressure systems in the equatorial Indian Ocean and migrate northward (Krishna 2009, Ng and Chan 2012) and this was also the case with Fani. After its genesis, Fani tracked northward into the high-aerosol area and its interaction with the aerosols is visible in the swirling patterns of AOT of sulfate (figure 1(b)). Meanwhile, the local SST anomaly at Fani's position reached as high as 2.5°C (figure 1(c)), which is in line with projections from the post-1980 warming trend of the BOB SST during May (Wang *et al* 2013).

The control simulation of Fani (CTL) in terms of daily precipitation and the 850hPa streamfunction at 00 UTC is plotted in figure 2 (middle column), alongside the aerosol removal simulation (RAERO, figure 2 right column). The WRF-Chem simulation captures the size and intensity of Fani in general, albeit overestimating the cyclone winds starting on April 29. The position of cyclone rainbands is slightly offset day-by-day, while the accumulated precipitation amounts within 12° lat. \times 12° long. around the cyclone center averaged to an underestimation of $\sim 15\%$ during the 5 d, based on CTL (figure 3(d)). A comparison of Fani's observed and modeled trajectories is plotted in figure 3(a) for CTL and in figure 3(b) with other experiments, following the 850 hPa vorticity center. Despite the sub-daily variation in the trajectory, the simulated cyclone track is generally in good agreement with the observed one, until 12Z April 30 when the CTL track persistently deviated east by about 90 km.

Acknowledging this track bias, we next examined the differences in the 850 hPa geopotential height (HGT) between the control simulation and the other experiments to represent Fani's intensity (figure 3(c)), averaged within 12° lat. \times 12° long. around the cyclone center. Not surprisingly, the removal of the trends in the air and SST (DALL; olivedrab line) results in the strongest increase in cyclone pressure, signifying a reduction in Fani's strength, with the air

temperature's warming trend accounting for approximately two-thirds of the cyclone reduction (DAIR) and the SST trend accounting for one-third (DSST). The removal of aerosol (cyan line; RAERO) intensified the tropical cyclone initially, but then weakened it near landfall (May 1).

This result suggests that the effect of the BOB aerosols on Fani is relatively weak compared to that of the air temperature and SST trends, which could be attributed to greenhouse gases induced warming (Wang *et al* 2013). In terms of precipitation (figure 3(d); averaged within the 12° lat. \times 12° long. box following Fani), the outcome of the simulations agrees with that of the 850 hPa HGT. The removal of both the air temperature and SST trends (DALL) resulted in a reduction of cyclone precipitation by about 51% during 4/28-5/2, in which the tropospheric warming shows almost twice as strong an effect on Fani (39% reduction) as that of SST warming (22% reduction). These results are consistent with Trenberth *et al* (2018) in that the increased SST not only enhances fuel available to sustain and intensify a hurricane but also increases its rains upon landfall. As shown in figures 3(d) and (e), DSST and DBSST_RAERO (detrend SST and double trend SST) generally decreased and increased precipitation, respectively. Note that the precipitation response to the detrended IC and BC is much quicker than the pressure field, showing differences at the first forecast hour of the simulations. The removal of aerosols (RAERO), on the other hand, does not show a robust net effect from 4/27-5/3.

Without aerosol and its direct and indirect effect with radiation and microphysics, the simulations with removed climate trends show a consistent tendency of a weakened Fani, with increased geopotential height and decreased precipitation of smaller amplitude. Comparison between DALL and DALL_RAERO suggests that aerosol interactions with the atmosphere act to mitigate the warming effect on Fani by reducing the 155 m increase in 850 hPa geopotential height to a smaller level of 138 m, and the 51% decrease in precipitation to 39% from the five-day average. In other words, Fani might have grown noticeably stronger if the BOB aerosols were not present. Likewise, by doubling the warming trends in the air and SST with the absence of aerosols (DBALL_RAERO), Fani would intensify with a drop of height by 11 m accompanied by a precipitation increase of 15% during 4/28-5/2; this sensitivity test shows the effect of amplified warming and lends support to the detrend simulations.

Any change in the cyclone intensity can affect its trajectory. As shown in figure 3(b), Fani would drift westward without the influence of post-1990 climate trends and the presence of aerosols. Likewise, with further (doubled) warming in the atmosphere, the cyclone would drift eastward. The uncertainty of aerosol effect in the ensemble CTL with respect

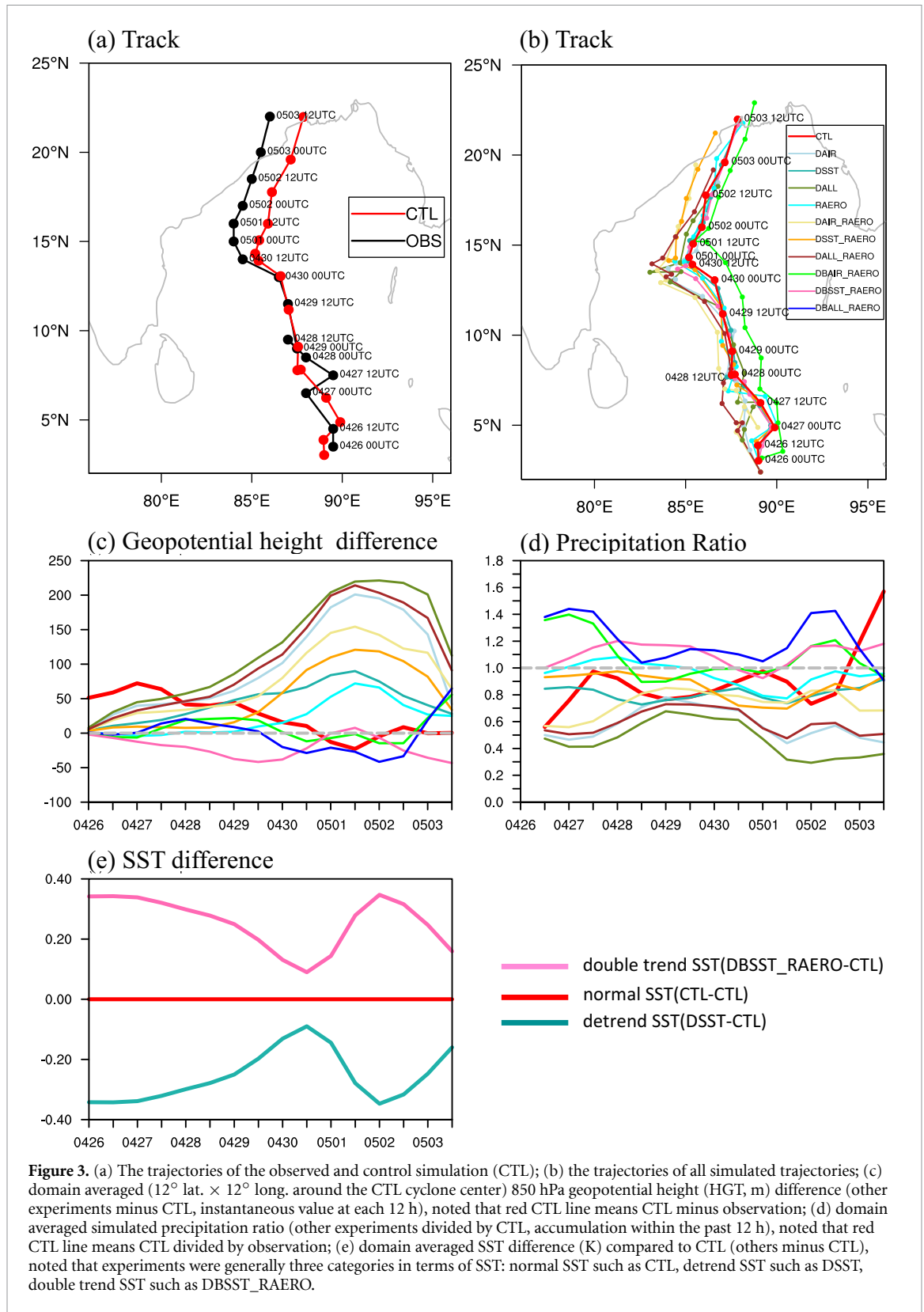


Figure 3. (a) The trajectories of the observed and control simulation (CTL); (b) the trajectories of all simulated trajectories; (c) domain averaged (12° lat. \times 12° long. around the CTL cyclone center) 850 hPa geopotential height (HGT, m) difference (other experiments minus CTL, instantaneous value at each 12 h), noted that red CTL line means CTL minus observation; (d) domain averaged simulated precipitation ratio (other experiments divided by CTL, accumulation within the past 12 h), noted that red CTL line means CTL divided by observation; (e) domain averaged SST difference (K) compared to CTL (others minus CTL), noted that experiments were generally three categories in terms of SST: normal SST such as CTL, detrend SST such as DSST, double trend SST such as DBSST_RAERO.

Table 1. CTL experiments of WRF-Chem at 4 km grid spacing.

Experiments	PBL schemes	Microphysics schemes
CTL	YSU_MOR	Morrison
	YSU_LIN	Lin
	MYNN_MOR	Lin
	MYNN_LIN	Morrison

Table 2. Description of all the WRF-Chem experiments.

Experiments		Descriptions
Control experiment	CTL	simulation with original IC and BC for all tropospheric variables from GFS data; consideration of the inclusion of the anthropogenic aerosol effects, including aerosol and its direct and indirect effect with atmospheric radiation and microphysics
	DAIR	same as CTL but remove the linear monthly trends of post-1990 from NCEP R2 for the IC and BC for all tropospheric variables
Detrend experiments	DSST	simulation as CTL but remove the linear monthly trends from the IC and BC for SST
	DALL	same as CTL but remove the linear monthly trends of post-1990 from NCEP R2 for the IC and BC for both SST and tropospheric variables
No aerosol experiment	RAERO	simulation with original IC and BC for all tropospheric variables from GFS data; without aerosol forcing and turn off aerosol direct and indirect effect, basically it is WRF model.
	DAIR_RAERO	same as RAERO, simulation removed the linear monthly trends of post-1990 from NCEP R2 for the IC and BC for all tropospheric variables; without aerosol forcing and turn off aerosol direct and indirect effect
	DSST_RAERO	same as RAERO, simulation removed the linear monthly trends of post-1990 from NCEP R2 for the IC and BC for SST; without aerosol forcing and turn off aerosol direct and indirect effect
Detrend experiments and without aerosol	DALL_RAERO	same as RAERO, simulation removed the linear trends from the IC and BC for both SST and tropospheric variables; without aerosol forcing and turn off aerosol direct and indirect effect
	DBAIR_RAERO	same as RAERO, simulation removed the linear monthly trends of post-1990 from NCEP R2 for the IC and BC for all tropospheric variables instead of removed; without aerosol forcing and turn off aerosol direct and indirect effect
	DBSST_RAERO	same as RAERO, simulation removed the linear monthly trends of post-1990 from NCEP R2 for the IC and BC for SST instead of removed; without aerosol forcing and turn off aerosol direct and indirect effect
Double trend experiments and without aerosol	DBALL_RAERO	same as RAERO, simulation removed the linear monthly trends of post-1990 from NCEP R2 for the IC and BC for both SST and tropospheric variables instead of removed; without aerosol forcing and turn off aerosol direct and indirect effect

to different parameterization schemes (table 1) was assessed using the 4 km simulations, as shown in figures 4(a) and (b). By changing the PBL schemes to MYNN and the microphysics schemes to LIN, the different members produce a difference in the 850 hPa geopotential height that is more noticeable in the later period (after 4/30) than before, up to 100 m. The precipitation fluctuation is also more pronounced after 4/30 with a difference up to 5 mm 12 h⁻¹.

The ensemble size of TC simulations is important. Reed *et al* (2020) and Patricola and Wehner (2018) argued that an ensemble size of at least 10 is necessary for TC attribution experiments. Here, we conducted twelve more simulations using a 24 km grid spacing by following the experiments in table 2 through the combination of three cumulus schemes and two different microphysics

schemes and two different PBL schemes, which are described in table 3 and named with 24 km (figure 4). Together with the 4 km cloud-resolving simulations, we produced an ensemble size of 13 for each experiment. Based on the median of 850 hPa geopotential height difference in CTL_24 km relative to CTL (figure 4(c)), the ensemble of simulations appears to overestimate Fani by about 58 m in terms of the 850 hPa HGT. Meanwhile, other 24 km simulations uniformly experienced an intensification of Fani's geopotential height within the range from -11 m (DSST_RAERO_24 km) to -45 m (DBALL_RAERO_24 km). In other words, the coarser-resolution simulations are in general agreement with the convection-permitting ones, suggesting aerosol invigoration achieved by the two-way interaction between convection and microphysics

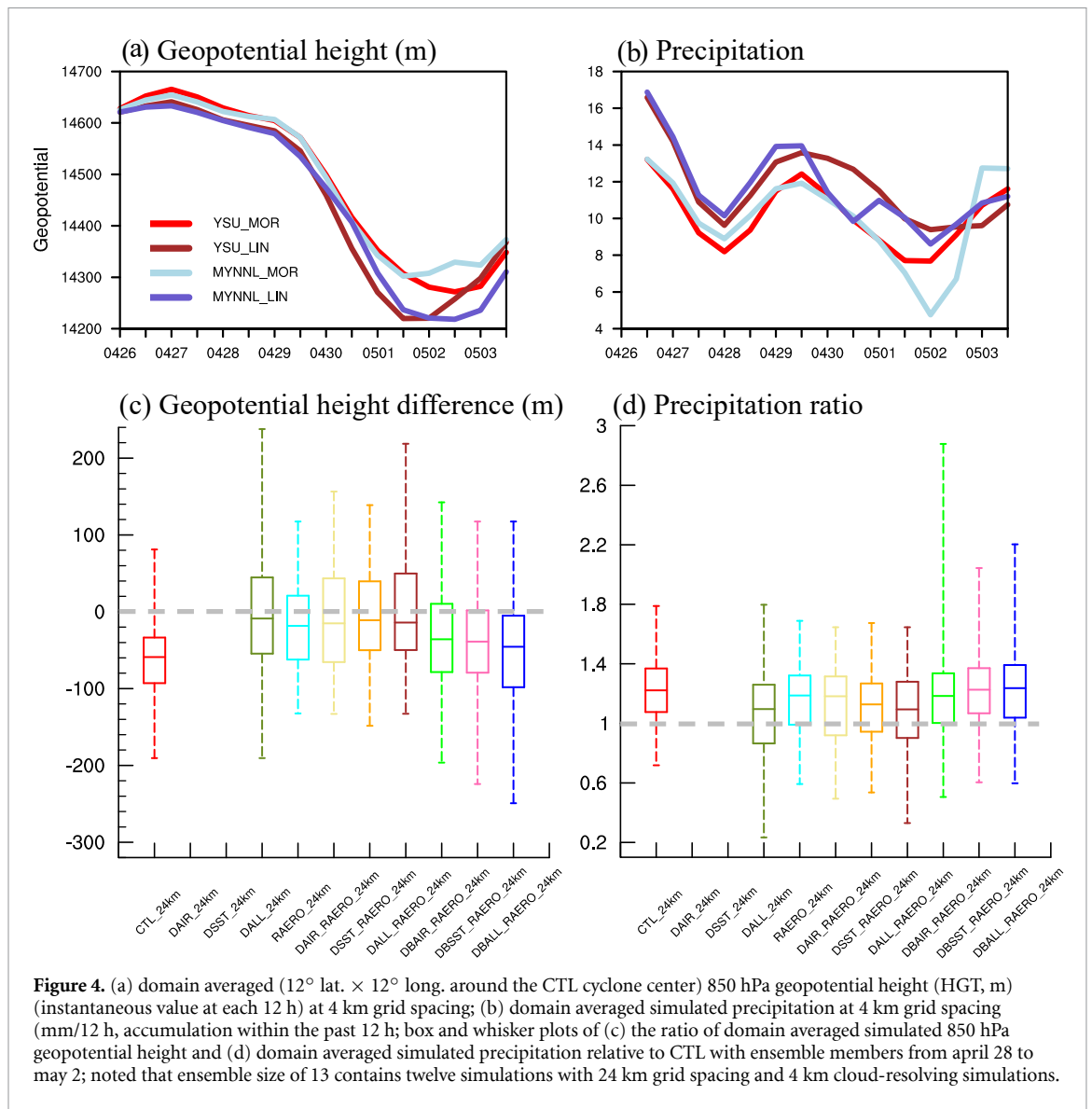


Table 3. Twelve combination of paramutation schemes of WRF-Chem at 24 km grid spacing for all runs in table 2.

Combinations	Cumulus schemes	PBL schemes	Microphysics schemes
1	Kain-Fritsch (Kain 2004)	YSU	Morrison
2	Kain-Fritsch	YSU	Lin
3	Kain-Fritsch	MYNN	Morrison
4	Kain-Fritsch	MYNN	LIn
5	Betts-Miller-Janjic (Janjic 1994)	YSU	Morrison
6	Betts-Miller-Janjic	YSU	Lin
7	Betts-Miller-Janjic	MYNN	Morrison
8	Betts-Miller-Janjic	MYNN	LIn
9	Grell-3 (Grell and Dévényi 2002)	YSU	Morrison
10	Grell-3	YSU	Lin
11	Grell-3	MYNN	Morrison
12	Grell-3	MYNN	LIn

interaction might be weaker in the case of Fani. It is likely due to the highly saturated aerosol in the BOB compared to other regions.

In terms of the accumulated precipitation, figure 4(d) shows the precipitation ratio compared to CTL during the 5 d. According to the median, CTL_24 km

increased precipitation by 22%. By comparing the detrend + aerosol experiments (DAIR_24 km, DSST_24 km, and DALL_24 km) with the aerosol removal simulations (DAIR_RAERO_24 km, DSST_RAERO_24 km, and DALL_RAERO_24 km), the accumulated precipitation was increased up to

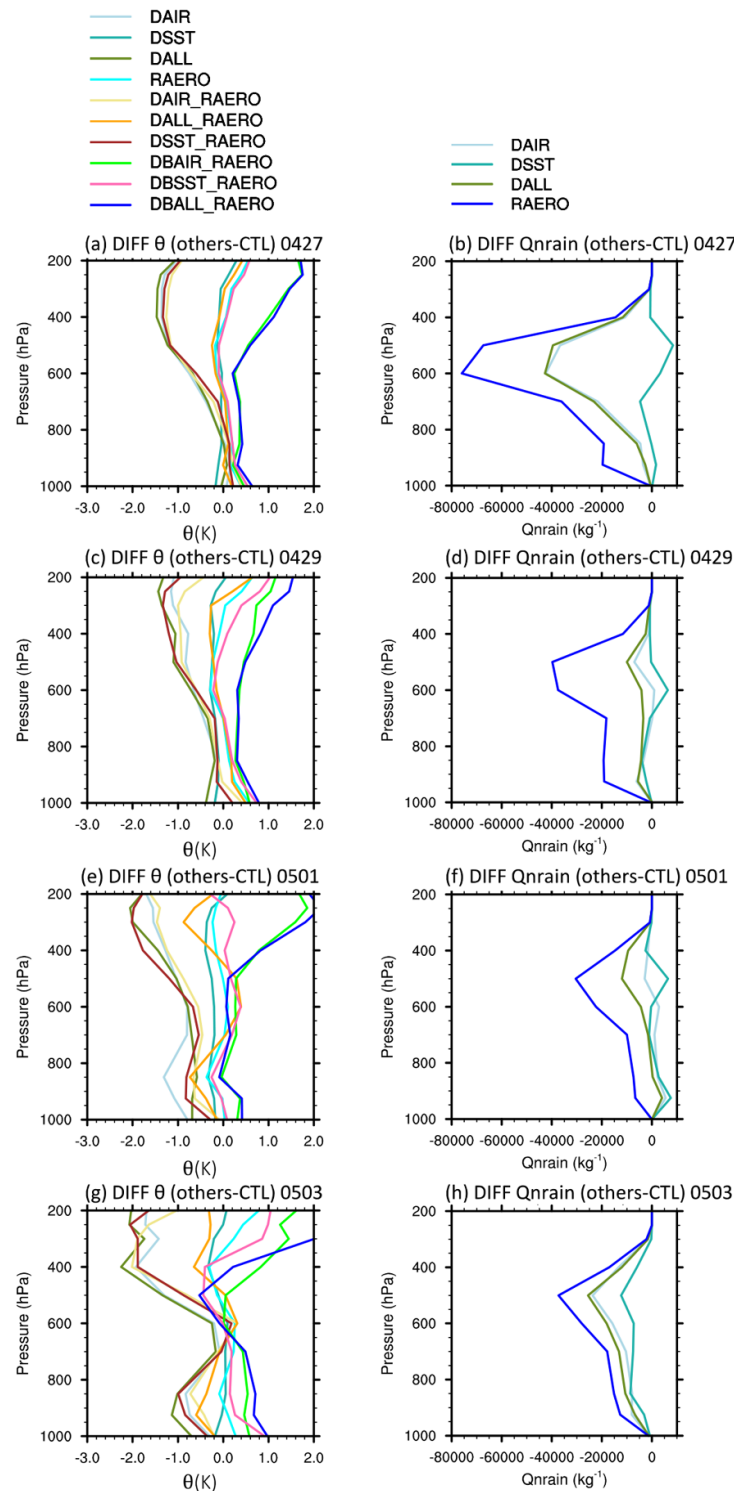


Figure 5. The vertical profile of the domain averaged (12° lat. \times 12° long. around the CTL cyclone center) potential temperature (θ , K) and raindrops number concentration (Qrain, kg^{-1}) difference (other experiments minus CTL): (a), (c), (e) and (g) are potential temperature difference; (b), (d), (f) and (h) are rain number concentration difference.

6%. These ensemble results suggest that aerosol plays a negative effect on cyclone Fani by weakening its strength and precipitation. The double trend experiments profoundly increased the accumulated precipitation at a range of 18%–23%. Therefore, despite the uncertainty introduced by different model settings, Fani underwent an intensification effect from warming trend (which is mostly warming)

accompanied by a weakening effect from anthropogenic aerosols (but less pronounced than warming). These results echo the finding of (Sobel *et al* 2019) regarding TC potential intensity but differ in that climate warming intensifies a TC more so than aerosols reduce it, at least in the BOB. Reasons of the apparent discrepancy with those of (Sobel *et al* 2019) are manifold. In the regional model (WRF-Chem),

SST is ingested from the GFS forcing data and therefore does not undergo the atmosphere feedback as in the fully coupled global model. The physics schemes, gaseous chemistry and aerosol mechanism all differ between the global and regional models. Moreover, the different resolutions and aerosol components can lead to somewhat different simulation results.

5. In-cyclone mechanisms

The processes by which the different experiments produced different amounts of precipitation from Fani are discussed as follows. The removal of aerosol interactions did not produce as much of a change in the potential temperature as the other detrend simulations did (figure 5 left column). Most of the detrend simulations produced two stabilization zones, one in the lower troposphere since most of the atmospheric warming took place in the lower levels (not shown), and the other in the upper troposphere, corresponding to the reduced convective precipitation (cf figure 3(d)) and an associated reduction in latent heat release (not shown). Likewise, the double-warming runs without aerosol interactions destabilize the lower troposphere while warming the upper troposphere through enhanced deep convection. Meanwhile, the effect of anthropogenic aerosols is not consistent, at least between April 27 and May 1; this echoes the fluctuated precipitation difference in figure 3(d).

By plotting the vertical profile of the concentration of raindrops ('qnrain' in WRF-Chem) within the 12° domain centered on Fani, the simulations without engaging the aerosol and its direct and indirect effect (experiments named with RAERO) produced a consistent reduction in the concentration of raindrops, particularly in the middle troposphere (figure 5 right column). This reduction in 'qnrain' echoes the previous simulations of (May *et al* 2011) and (Hassim *et al* 2016), who found decreased number concentrations of smaller rain droplets in the core of convective storms during high aerosol conditions and the resultant decline in the deposition growth of cloud ice crystals. Such an effect of anthropogenic aerosols is different from that of sea-salt aerosols, which can strengthen a tropical cyclone through enhancing the condensation process (Jiang *et al* 2019). (Note that all the detrend simulations with the aerosol module turned off produced the same result in 'qnrain', hence the single profile of RAERO.) The detrend experiments with an active aerosol interaction suggest that the atmospheric warming trend mitigates the weakening effect of anthropogenic aerosols on the concentration of raindrops by ~50%, while the SST trend (or the combination of air and SST trends) completely offset that weakening

effect, hence delineating a 'tug of war' in their respective effects on Fani.

We should note that the selected domain size for evaluation may influence the intensity of precipitation since more intense rainfall occurs closer to Fani's center. By checking the vertical profile of 'qnrain' within 6° domain centered on Fani (not shown), despite more intense rainfall as expected, the variance of 'qnrain' profile is consistent with 12° x 12° domain box centered on Fani. These analyses suggest that anthropogenic aerosols affected Cyclone Fani primarily by modulating the raindrop concentration, while climate trends modulated Fani mainly through changing the atmospheric instability.

6. Concluding remarks

Through the present WRF-Chem simulations, the removal of warming trends from the troposphere and SST appears to reduce Fani's intensity and decrease the cyclone precipitation, while the removal of aerosol interactions in the simulation initially strengthened the tropical cyclone, but later weakened it. However, when aerosols and climate trends were both removed from the simulations, the intensification effect of regional/BOB aerosols and climate warming on Fani (DALL_RAERO) was 'mitigated' by over 49% during April 28-May 2, suggesting certain non-linear dynamics involved in the aerosol interactions with the increased heat in the air and ocean. An assessment could be made, based on the cyclone precipitation ratio averaged from April 28 to May 2 (figure 3(d)), that the removal of post-1990 regional climate warming alone (while keeping the aerosol effects; DALL) could have increased Fani's precipitation by 51%, from which aerosols would deduct up to 13%. This leaves the net intensification of Fani due to the BOB climate warming and aerosol combined effects to be about 38%. This result provides a rudimentary, yet quantitative estimate for what a premonsoon TC like Fani might have been like had it developed in the pre-1990 atmospheric and oceanic conditions and without the presence of anthropogenic aerosols.

Caution should be exercised when interpreting these statements since the simulations presented here did have drawbacks. First, the cloud resolving (4 km) simulations were not done in a large-ensemble fashion. The challenge lies in that setting up the interactive aerosol module of high-resolution WRF-Chem for large ensembles that involve engaging various physics schemes and different resolutions in the detrend experiments is extremely difficult, for the model would become unstable. As a result, model sensitivity and uncertainty have not been fully evaluated (such as the effect of the ensemble choices on Fani tracks). Second, the regional climate warming effect was estimated in terms of the 'change' in the air and SST, while the aerosols effect was examined in

a ‘with or without’ manner, so the two effects were not analyzed symmetrically. Third, one should expect that the simulation results may fluctuate by changing the period of climate trends and/or using a different model. Finally, one should consider the long-term effect of the persistent increase in anthropogenic aerosols on the intensification of the pre-monsoon trough of the BOB, a trend that has modified the pre-monsoon tropical cyclone activity including frequency and intensity (Wang et al 2013).

Amid the model uncertainty, the simulations conducted and presented here call for future efforts with more sophisticated models in understanding how the rapidly increasing anthropogenic aerosols in the BOB interact with the pronounced warming in producing the compound effects on high-impact tropical cyclones like Fani.

Acknowledgments

LZ is supported by the Strategic Priority Research Program of the Chinese Academy of Sciences (XDA2006010202), the National Natural Science Foundation of China (41930759, 41822501, 41975012, 91837209, 41605011, 41975130, 41875016, 41875018), and the Youth Innovation Promotion Association of CAS (QCH2019004). SYSW is supported by the US Department of Energy under Award Number DE-SC0016605 and the U.S. SERDP Project Number RC-2709. JHY is supported by GIST Research Institute IERI grant funded by the GIST in 2020 and the National Research Foundation of Korea under Grant NRF_2017R1A2B4007480. Surface wind data in Figure 1b is derived from GFS data provided by EMC/NCEP/NWS/NOAA, while current data in Figure 1c is derived from WAVEWATCH III data provided by MMAB/EMC/NCEP/NWS/NOAA, displayed by <https://earth.nullschool.net>.

Data availability statement

The data that support the findings of this study are available upon request from the authors.

ORCID iDs

Lin Zhao  <https://orcid.org/0000-0002-6520-5096>
S-Y Simon Wang  <https://orcid.org/0000-0003-2009-2275>

Jin-Ho Yoon  <https://orcid.org/0000-0002-4939-8078>

References

- Ackermann I J, Hass H, Memmesheimer M, Ebel A, Binkowski F S and Shankar U 1998 Modal aerosol dynamics model for Europe: development and first applications *Atmos. Environ.* **32** 2981–99
- Altaratz O, Koren I, Remer L and Hirsch E 2014 Cloud invigoration by aerosols—coupling between microphysics and dynamics *Atmos. Res.* **140** 38–60
- Bhat G, Gadgil S, Hareesh Kumar P, Kalsi S, Madhusoodanan P, Murty V, Prasada Rao C, Babu V R, Rao L and Rao R 2001 BOBMEX: the Bay of Bengal monsoon experiment *Bull. Am. Meteorol. Soc.* **82** 2217–44
- Campana K et al 2019 The development and success of NCEP’s global forecast system *99th American Meteorological Society Annual Meeting (AMS) (January)*
- Chen F and Dudhia J 2001 Coupling an advanced land surface–hydrology model with the Penn state–NCAR MM5 modeling system. Part I: Model implementation and sensitivity *Mon. Weather Rev.* **129** 569–85
- Cho C, Li R, Wang S-Y, Yoon J-H and Gillies R R 2016 Anthropogenic footprint of climate change in the June 2013 northern India flood *Clim. Dyn.* **46** 797–805
- Evan A T, Kossin J P and Ramanathan V 2011 Arabian Sea tropical cyclones intensified by emissions of black carbon and other aerosols *Nature* **479** 94–97
- Fan J, Rosenfeld D, Zhang Y, Giangrande S E, Li Z, Machado L A, Martin S T, Yang Y, Wang J and Artaxo P 2018 Substantial convection and precipitation enhancements by ultrafine aerosol particles *Science* **359** 411–8
- Fan J, Wang Y, Rosenfeld D and Liu X 2016 Review of aerosol–cloud interactions: mechanisms, significance, and challenges *J. Atmos. Sci.* **73** 4221–52
- Fu H and Wang Y 2018 Effect of uncertainties in sea surface temperature dataset on the simulation of typhoon Nangka (2015) *Atmos. Sci. Lett.* **19** e797
- Fu Q and Liou K 1992 On the correlated k-distribution method for radiative transfer in nonhomogeneous atmospheres *J. Atmos. Sci.* **49** 2139–56
- Grell G A and Dévényi D 2002 A generalized approach to parameterizing convection combining ensemble and data assimilation techniques *Geophys. Res. Lett.* **29** 38-1-38-4
- Grell G A, Peckham S E, Schmitz R, Mckeen S A, Frost G, Skamarock W C and Eder B 2005 Fully coupled “online” chemistry within the WRF model *Atmos. Environ.* **39** 6957–75
- Gu Y, Liou K, Ou S and Fovell R 2011 Cirrus cloud simulations using WRF with improved radiation parameterization and increased vertical resolution *J. Geophys. Res. Atmos.* **116** D06119
- Hassim M, Grabowski W and Lane T 2016 Impact of aerosols on precipitation over the maritime continent simulated by a convection-permitting model *Atmos. Chem. Phys. Discuss.* **1**–25
- Hazra A, Goswami B and Chen J-P 2013 Role of interactions between aerosol radiative effect, dynamics, and cloud microphysics on transitions of monsoon intraseasonal oscillations *J. Atmos. Sci.* **70** 2073–87
- Hoarau K, Bernard J and Chalonge L 2012 Intense tropical cyclone activities in the northern Indian Ocean *Int. J. Clim.* **32** 1935–45
- Hong S-Y, Noh Y and Dudhia J 2006 A new vertical diffusion package with an explicit treatment of entrainment processes *Mon. Weather Rev.* **134** 2318–41
- Janjić Z I 1994 The step-mountain eta coordinate model: further developments of the convection, viscous sublayer, and turbulence closure schemes *Mon. Weather Rev.* **122** 927–45
- Janssens-Maenhout G, Crippa M, Guizzardi D, Dentener F, Muntean M, Pouliot G, Keating T, Zhang Q, Kurokawa J and Wankmüller R 2015 HTAP_v2. 2: a mosaic of regional and global emission grid maps for 2008 and 2010 to study hemispheric transport of air pollution *Atmos. Chem. Phys.* **15** 11411–32
- Jiang B, Lin W, Li F and Chen B 2019 Simulation of the effects of sea-salt aerosols on cloud ice and precipitation of a tropical cyclone *Atmos. Sci. Lett.* **20** e936
- Jiang J H, Su H, Huang L, Wang Y, Massie S, Zhao B, Omar A and Wang Z 2018 Contrasting effects on deep convective clouds by different types of aerosols *Nat. Commun.* **9** 3874

- Kain J S 2004 The Kain–Fritsch convective parameterization: an update *J. Appl. Meteorol.* **43** 170–81
- Kanamitsu M, Ebisuzaki W, Woollen J, Yang S-K, Hnilo J, Fiorino M and Potter G 2002 Ncep–doe amp–ii reanalysis (r-2) *Bull. Am. Meteorol. Soc.* **83** 1631–44
- Krishna K M 2009 Intensifying tropical cyclones over the North Indian ocean during summer monsoon—global warming *Glob. Planet Change* **65** 12–16
- Landsea C W, Harper B A, Hoarau K and Knaff J A 2006 Can we detect trends in extreme tropical cyclones? *Science* **313** 452–4
- Lau W K and Kim K M 2007 How nature foiled the 2006 hurricane forecasts *Eos Trans. Am. Geophys. Union* **88** 105–7
- Lenderink G, Barbero R, Loriaux J and Fowler H 2017 Super-clausius–clapeyron scaling of extreme hourly convective precipitation and its relation to large-scale atmospheric conditions *J. Clim.* **30** 6037–52
- Lin Y-L, Farley R D and Orville H D 1983 Bulk parameterization of the snow field in a cloud model *J. Clim. Appl. Meteorol.* **22** 1065–92
- May P, Bringi V and Thurai M 2011 Do we observe aerosol impacts on DSDs in strongly forced tropical thunderstorms? *J. Atmos. Sci.* **68** 1902–10
- Morrison H, Thompson G and Tatarskii V 2009 Impact of cloud microphysics on the development of trailing stratiform precipitation in a simulated squall line: comparison of one- and two-moment schemes *Mon. Weather Rev.* **137** 991–1007
- Nakanishi M and Niino H 2006 An improved Mellor–Yamada level-3 model: its numerical stability and application to a regional prediction of advection fog *Bound.-Layer Meteorol.* **119** 397–407
- Ng E K and Chan J C 2012 Interannual variations of tropical cyclone activity over the north Indian Ocean *Int. J. Clim.* **32** 819–30
- Patricola C M and Wehner M F 2018 Anthropogenic influences on major tropical cyclone events *Nature* **563** 339–46
- Powers J G, Klemp J B, Skamarock W C, Davis C A, Dudhia J, Gill D O, Coen J L, Gochis D J, Ahmadov R and Peckham S E 2017 The weather research and forecasting model: overview, system efforts, and future directions *Bull. Am. Meteorol. Soc.* **98** 1717–37
- Reale O, Lau K, Da Silva A and Matsui T 2014 Impact of assimilated and interactive aerosol on tropical cyclogenesis *Geophys. Res. Lett.* **41** 3282–8
- Reed K, Stansfield A, Wehner M and Zarzycki C 2020 Forecasted attribution of the human influence on Hurricane Florence *Sci. Adv.* **6** eaaw9253
- Reynolds R W, Smith T M, Liu C, Chelton D B, Casey K S and Schlax M G 2007 Daily high-resolution-blended analyses for sea surface temperature *J. Clim.* **20** 5473–96
- Risser M D and Wehner M F 2017 Attributable human-induced changes in the likelihood and magnitude of the observed extreme precipitation during hurricane harvey *Geophys. Res. Lett.* **44** 12457–64
- Rosenfeld D, Woodley W L, Khain A, Cotton W R, Carrió G, Ginis I and Golden J H 2012 Aerosol effects on microstructure and intensity of tropical cyclones *Bull. Am. Meteorol. Soc.* **93** 987–1001
- Skamarock W C, Klemp J B, Dudhia J, Gill D O, Barker D M, Duda M G, Huang X-Y, Wang W and Powers J G 2008 *A Description of the Advanced Research WRF Version 3*, NCAR Technical Note (Boulder, CO, USA: National Center for Atmospheric Research)
- Sobel A H, Camargo S J and Previdi M 2019 Aerosol versus greenhouse gas effects on tropical cyclone potential intensity and the hydrologic cycle *J. Clim.* **32** 5511–27
- Takayabu I, Hibino K, Sasaki H, Shiogama H, Mori N, Shibutani Y and Takemi T 2015 Climate change effects on the worst-case storm surge: a case study of Typhoon Haiyan *Environ. Res. Lett.* **10** 064011
- Tao W K, Chen J P, Li Z, Wang C and Zhang C 2012 Impact of aerosols on convective clouds and precipitation *Rev. Geophys.* **50** RG2001
- Trenberth K E, Cheng L, Jacobs P, Zhang Y and Fasullo J 2018 Hurricane Harvey links to ocean heat content and climate change adaptation *Earth's Future* **6** 730–44
- Van Oldenborgh G J, Van Der Wiel K, Sebastian A, Singh R, Arrighi J, Otto F, Haustein K, Li S, Vecchi G and Cullen H 2017 Attribution of extreme rainfall from Hurricane Harvey, august 2017 *Environ. Res. Lett.* **12** 124009
- Varble A 2018 Erroneous attribution of deep convective invigoration to aerosol concentration *J. Atmos. Sci.* **75** 1351–68
- Wang S S, Zhao L, Yoon J-H, Klotzbach P and Gillies R R 2018 Quantitative attribution of climate effects on Hurricane Harvey's extreme rainfall in Texas *Environ. Res. Lett.* **13** 054014
- Wang S Y, Buckley B M, Yoon J H and Fosu B 2013 Intensification of premonsoon tropical cyclones in the Bay of Bengal and its impacts on Myanmar *J. Geophys. Res. Atmos.* **118** 4373–84
- Wang S Y S, Zhao L and Gillies R R 2016 Synoptic and quantitative attributions of the extreme precipitation leading to the August 2016 Louisiana flood *Geophys. Res. Lett.* **43** 11805–14
- Wehner M F, Reed K A and Zarzycki C M 2017 *High-resolution Multi-decadal Simulation of Tropical Cyclones. Hurricanes and Climate Change* (Berlin: Springer) pp 187–211
- Yu J and Wang Y 2009 Response of tropical cyclone potential intensity over the north Indian Ocean to global warming *Geophys. Res. Lett.* **36** L03709
- Zappa G and Shepherd T G 2017 Storylines of atmospheric circulation change for European regional climate impact assessment *J. Clim.* **30** 6561–77
- Zaveri R A and Peters L K 1999 A new lumped structure photochemical mechanism for large-scale applications *J. Geophys. Res. Atmos.* **104** 30387–415